$Cs_3Zr_7Cl_{20}Mn$: A Zirconium Cluster Network Compound with Isolated $ZrCl_5^-$ Units in a Stuffed Perovskite Structure

Jie Zhang and John D. Corbett*

Department of Chemistry, Iowa State University, Ames, Iowa 50011

Received November 1, 1994[⊗]

Reactions of Zr, $ZrCl_4$, and $MnCl_2$ in welded Ta containers at 800 °C produce the title phase in major amounts. A comparable electronic and structural configuration is also found with interstitial boron, but not in isostructural compounds with other interstitial or alkali metal atoms. The crystal structure of $Cs_3(ZrCl_5)[Zr_6(Mn)Cl_{12}]Cl_{6/2}$ was established by single-crystal diffraction ($R\bar{3}c$, $Z = 6$, $a = 12.8924$ (1) Å, $c = 35.187$ (6) Å, $R/R_w = 1.9/2.3\%$ for 920 data to $2\theta = 60°$). The structure contains a three-dimensional array of 18-electron $Zr_6(Mn)Cl_{12}$ clusters interbridged by 6/2 $Cl^{a\text{-}a}$ atoms at zirconium vertices. This represents a sixth independent structure type for M_6X_{15} bridged cluster networks. The structure derives from a ReO_3-like primitive lattice of the cubic Nb_6F_{15} structure with linear bridges that has been given a "trigonal twist" about [111] to form a rhombohedral (tilted) perovskite arrangement with the novel $ZrCl_5^-$ at the body center. This new D_{3h} anion does not share halogen with the rest of the structure and appears to be stabilized by a particularly good fit within the network. A double ccp cluster arrangement along c_H provides for a coherent intercluster bridging arrangement. The cesium cations necessitated by the anionic network and by the $CsZrCl_5$ component are bound in well-suited 12-coordinate sites among the chlorines.

Introduction

Solid ternary or quaternary compounds containing zirconium halide clusters of the Zr_6X_{12} type (X = Cl, Br, I) apparently always contain an interstitial element Z in each cluster, one that is, except for Z = H, always centered. The structures also reveal that additional bifunctional ligands, usually X, are always bonded exo at every zirconium vertex. The versatility possible with these variables and the inclusion of countercations turns out to be large indeed, particularly for the chlorides. All fall within the description $A_x[Zr_6(Z)Cl^i_{12}]Cl^a_n$ where examples have been found with $0 \le n \le 6$ additional outer halides bonded at the exo positions and $0 \le x \le 6$ cations A, usually alkali metals, in the intercluster regions within halide polyhedra. The variety of phases collectively reflect the many ways in which closed-shell electronic configurations of the clusters may be achieved.[1,2]

A particularly diverse range of structures have been discovered with $n = 3$, that is, with $(Zr_6(Z)X_{12})X_{6/2}$ (X = Cl, Br) networks in which the three $X^{a\text{-}a}$ atoms interbridge the cluster cores at all vertices. The number of independent structure types known for these $(M_6X_{12})X_{6/2}$ networks, that is, with different bridge angularities, ring sizes, and connectivities such that they cannot be interconverted except by bond breakage,[3−5] has recently been increased to 5 by the addition of the $Rb_5Zr_6Br_{15}$-Be tunnel structure.[6] This article and the following one[7] report two related examples of yet another version, this one based on a single primitive lattice of the interpenetrating pairs that are present in the cubic Nb_6F_{15} structure.[8] Each lattice therein is equivalent to the ReO_3 structure, with $[M_6X_{12}Z]$ clusters substituting for Re and bridging halogen $X^{a\text{-}a}$ for oxygen, that has been further collapsed or twisted and filled with counterions to give perovskite-like derivatives. The present $Cs_3Zr_7Cl_{20}Mn$ example, better described as $Cs_3(ZrCl_5)Zr_6Cl_{15}Mn$, also contains the novel space-filling $ZrCl_5^-$ anion, while cesium cations partially fill the space occupied by $ZrCl_5^-$ in the following structures of $Cs_3Zr_6Br_{15}C$ and $Cs_{3.4}Zr_6Br_{15}B$.[7] Manganese is the lightest transition metal that has been encapsulated within Zr_6Cl_{12}-type clusters, heretofore only in two examples, $Li_2Zr_6Cl_{15}Mn$, which can be described as a stuffed version of Nb_6F_{15} or, better, of $Zr_6Cl_{15}Co$,[5] and the more pervasive structure type of $LiZr_6Cl_{14}Mn$.[9]

Experimental Section

The quality of the starting materials, the syntheses and purification of $ZrCl_4$ and powdered Zr, the reaction techniques utilizing welded Ta containers, and Guinier diffraction and analysis procedures have all been described before.[10] Sublimed $MnCl_2$ was employed as the interstitial source, this originating with $MnCl_2{\cdot}4H_2O$ (Baker, reagent) that was first refluxed with liquid $SOCl_2$. All reactants and products were handled only in a high-quality glovebox. The phase distributions within/purities of the products were in all cases estimated on the basis of observed Guinier powder patterns vs those calculated for appropriate compositions in known structures.

Syntheses. Powdered $Cs_3(ZrCl_5)Zr_6Cl_{15}Mn$ was first observed as an unknown phase produced in reactions (at either 850 °C for 4 weeks or 800−750 °C for 2 weeks) that were designed to synthesize the hypothetical phase $Cs_2Zr_6Cl_{15}Mn$,[11] which was supposed to be related to $KCsZr_6Cl_{15}B$[3] or $K_2Zr_6Cl_{15}B$.[4] The new phase was obtained as the major product (>50%) together with the relatively stable and persistent $CsZr_6Cl_{14}Mn$,[9] ZrCl, and Cs_2ZrCl_6. Similar reactions repeated at higher temperatures in order to acquire single crystals showed that all Mn-containing cluster phases decompose above about 920 °C to give only simple compounds such as Cs_2ZrCl_6, $ZrCl_4$, and ZrCl. On the other hand, a reaction run under a temperature gradient (900−850 °C, 6

[⊗] Abstract published in *Advance ACS Abstracts,* March 1, 1995.

(1) Ziebarth, R. P.; Corbett, J. D. *Acc. Chem. Res.* **1989**, *22*, 256.
(2) Corbett, J. D. In *Modern Perspectives in Inorganic Crystal Chemistry*; Parthé, E., Ed.; Kluwer Academic Publishers: Dordrecht, The Netherlands, 1992; p 27.
(3) Ziebarth, R. P.; Corbett, J. D. *J. Am. Chem. Soc.* **1987**, *109*, 4844.
(4) Ziebarth, R. P.; Corbett, J. D. *J. Am. Chem. Soc.* **1988**, *110*, 1132.
(5) Zhang, J.; Corbett, J. D. *Inorg. Chem.* **1991**, *30*, 431.
(6) Qi, R.-Y.; Corbett, J. D., *Inorg. Chem.* **1995**, *34*, 1646.
(7) Qi, R.-Y.; Corbett, J. D. *Inorg. Chem.* **1995**, *34*, 1657.
(8) Schäfer, H.; von Schnering, H.-G.; Niehues, K.-J.; Nieder-Vahrenholz, H. G. *J. Less-Common Met.* **1965**, *9*, 95.
(9) Zhang, J.; Corbett, J. D. *J. Solid State Chem.* **1994**, *109*, 265.
(10) Zhang, J.; Corbett, J. D. *Inorg. Chem.* **1993**, *32*, 1566.
(11) Hughbanks, T.; Corbett, J. D. Unpublished research.

0020-1669/95/1334-1652$09.00/0

weeks) gave well crystallized $CsZr_6Cl_{14}Mn$ and the $Cs_3Zr_7Cl_{20}Mn$ sought. After the stoichiometry of the phase had been established by the X-ray study, efforts were made to improve the yield with the appropriate reactant proportions, but without success at 850 °C; rather, $CsZr_6Cl_{14}Mn$ and Cs_2ZrCl_6 were obtained as the main products after 6 weeks. A reaction at 800 °C (2 weeks) gave the target as the major phase, yet still mixed with $CsZr_6Cl_{14}Mn$ and Cs_2ZrCl_6. There appears to be some sort of equilibrium between the new $Cs_3(ZrCl_5)Zr_6Cl_{15}Mn$ salt and the simpler compounds; the stability of the $ZrCl_5^-$ component in the new structure vs $ZrCl_6^{2-}$ in the other product must be subtly dependent on the activity of chloride.

Attempts to expand the chemical variety of compounds with this structure had very limited success. The isostructural (and nominally isoelectronic) $Cs_3(ZrCl_5)Zr_6Cl_{15}B$ was found to have been obtained earlier as an unidentified phase in reactions aimed at $Cs_3Zr_6Cl_{16}B$ (850 °C, 20 days);[12] in contrast, the isomorph showed a very low contamination from the corresponding $CsZr_6Cl_{14}B$ and Cs_2ZrCl_6 (<10% total).

Other compounds with this structure have not been obtained, but this still leaves the possibility that the optimal conditions may not have been found. Attempts to substitute Cs^+ by Rb^+ resulted only in $RbZr_6Cl_{14}Mn$, or an unknown phase for the boron analogue, and Rb_2ZrCl_6. A similar reaction aimed at $K_3Zr_7Cl_{20}B$ yielded $KZr_6Cl_{14}B$ as the main product. Attempts to change the cluster interstitial to Cr (with A = Cs, Rb) or to Fe (Cs, K) were also negative, yielding unidentified phases in the former case (d_{max} < 6 Å) and $AZr_6Cl_{15}Fe$ (a superstructure related to $CsKZr_6Cl_{15}B$[3])[13] for the latter two systems. Possible replacement of the isolated Zr(IV) in $ZrCl_5^-$ with other cations of similar size to provide the analogous 18-electron cluster phases $Cs_3CuZr_6Cl_{20}Co$ and $Cs_3NbZr_6Cl_{20}Cr$ also yielded unknown phases with d_{max} < 6 Å in their patterns, probably noncluster compounds.

Structure Determination. The rod-shaped crystal used for the single-crystal study appeared black under reflected light and deep purplish red under transmitted light. Diffraction data were collected at room temperature on an Enraf-Nonius CAD4 diffractometer which, after proper transformation of the indexing, resulted in the correct *R*-centered hexagonal cell. Axial photographs revealed mirror planes perpendicular to $\bar{a}$ and $\bar{b}$ axes, indicating the Laue class was $R\bar{3}m$. Collection of the first 1200 reflections in one quadrant to $2\theta = 60°$ without systematic absence conditions confirmed the *R*-centering and the obverse setting. Six ψ-scans were also measured and averaged. No decay of standards was observed.

All data reduction, refinement, and mapping processes were carried out with the SDP package[14] and included anomalous dispersion corrections to the scattering factors. The processed data provided an additional observation condition and made $R3c$ or $R\bar{3}c$ the only possible space groups. The observed data ($3\sigma_I$ cutoff) averaged in Laue class $R\bar{3}m$ with $R_{ave} = 3.3\%$.

Although direct methods (SHELXS-86[15]) did not provide a plausible solution in $R\bar{3}c$, the one for $R3c$ was very promising. Refinement with standard procedures resulted in the correct model, a reasonable refinement with fair thermal parameters, and an essentially flat final difference map($\leq \pm 1$ e$^-$/Å^3). However, the result appeared to be close to centrosymmetric; a few atoms seemed to lie essentially on special positions in $R\bar{3}c$, e.g. *x*, 0, $^1/_4$, and the thermal parameters of several pairs of atoms were coupled, especially in the early stages of refinement. Refinement in $R\bar{3}c$ at this stage preserved the low agreement factors, small residual peaks in ΔF maps, and thermal ellipsoids with fair sizes and reasonable shapes. The occupancies of the two cation sites and the interstitial atom did not show significant deviations from 100% [Zr2 99.8(3)%, Cs 100.8(1)%, Mn 98.6(4)%] when both the multiplicity and thermal parameters were varied separately for each element, so these sites were each treated as fully occupied. Some important parameters of the data collection and refinement are listed in Table 1. Additional information as well as the anisotropic displacement parameters are given in the supplementary material, and these together with structure factor comparisons are also available from J.D.C.

Table 1. Crystallographic Data for $Cs_3Zr_7Cl_{20}Mn$

space group, *Z*	$R\bar{3}c$ (No. 167), 6	space group, *Z*	$R\bar{3}c$ (No. 167), 6
fw	1801.3	*t*, °C	21
a, Å[a]	12.8924(1)	μ, cm^{-1} (Mo Kα)	71.7
c, Å	35.187(6)	*R*,[b]%	1.9
V, Å^3	5067(1)	R_w,[b]%	2.3
d_{calc}, g cm^{-3}	3.542		

[a] From Guinier data with internal Si standard, λ = 1.540 562 Å. [b] $R = \sum||F_o| - |F_c||/\sum|F_o|$; $R_w = [\sum w(|F_o| - |F_c|)^2/\sum w(F_o)^2]^{1/2}$, $w = \sigma_F^{-2}$.

Table 2. Positional and Isotropic Displacement Parameters for $Cs_3(ZrCl_5)Zr_6Cl_{15}Mn$

		x	*y*	*z*	B_{eq},[a] Å^2
Zr1	36*f*	0.00605(3)	0.15526(3)	0.03995(1)	0.988(6)
Zr2	6*a*	0	0	$^1/_4$	1.66(1)
Cl1	36*f*	0.16505(8)	0.15871(8)	0.08461(3)	1.68(2)
Cl2	36*f*	0.32545(8)	0.15362(9)	0.00001(3)	1.60(2)
Cl3	18*e*	0.6553(1)	0	$^1/_4$	1.68(3)
Cl4	18*e*	0.1831(1)	0	$^1/_4$	2.44(4)
Cl5	12*c*	0	0	0.18048(5)	2.64(3)
Mn	6*b*	0	0	0	0.83(2)
Cs	18*d*	$^1/_2$	0	0	2.408(8)

[a] $B_{eq} = (8\pi^2/3)\sum_i\sum_j U_{ij}a_i^*a_j^*\bar{a}_i\bar{a}_j$.

Table 3. Important Distances (Å) and Angles (deg) in $Cs_3(ZrCl_5)Zr_6Cl_{15}Mn$

Distances					
Zr1−Mn	×1	2.4153(4)	Zr2−Cl4 (eq)	×3	2.361(1)
Zr1−Zr1	×2	3.4019(8)	Zr2−Cl5 (ax)	×2	2.446(2)
	×2	3.4296(7)	$\bar{d}$		2.395
$\bar{d}$		3.4156			
Zr−Cl1^i	×1	2.566(1)	Cs−Cl1	×2	3.582(1)
	×1	2.567(1)	Cs−Cl2	×2	3.667(1)
Zr−Cl2^i	×1	2.583(1)		×2	3.868(1)
	×1	2.588(1)	Cs−Cl3	×2	3.6814(6)
$\bar{d}$		2.576	Cs−Cl4	×2	3.5785(5)
Zr−Cl3$^{a\text{-}a}$	×1	2.7294(7)	Cs−Cl5	×2	3.7538(4)
			$\bar{d}$		3.688

Angles				
Zr1−Mn−Zr1	×1	180	Zr1−Cl3−Zr1	133.39(6)
	×2	89.54(1)	Mn−Zr1−Cl3	177.5(4)
	×2	90.46(1)		

Results and Discussion

Structure Description. The positional and isotropic-equivalent thermal parameters for $Cs_3(ZrCl_5)Zr_6Cl_{15}Mn$ are listed in Table 2. The generally more accurate cell dimensions that are obtained from Guinier powder diffraction analyses were employed in the calculation of distances and angles given in Table 3.

The rhombohedral structure of $Cs_3(ZrCl_5)Zr_6Cl_{15}Mn$ is composed of three main fragments, the $[Zr_6(Mn)Cl^i_{12}]Cl^{a\text{-}a}_{6/2}$ bridged network, the Cs^+ cations, and the novel counteranion $ZrCl_5^-$. A [110] projection is shown in Figure 1. The Mn-centered Zr_6 "octahedra" with $\bar{3}$ symmetry have all edges bridged by Cl^i and are interconnected by interbridging $Cl^{a\text{-}a}$. The ccp arrangement of clusters normal to [001], doubled in this case by the *c*-glide so as to produce clusters in the halves with opposite orientations, is common in rhombohedral arrangements, even when the clusters are not linked, as in $Ba_3Zr_6Cl_{18}Be$.[16] The present example is somewhat different in another respect though because the Cs cations (and the isolated Zr2) all lie within the fairly obvious close-packed layers defined mainly by chlorine. Other structure types generally have cations in suitable cavities between chlorine layers as well.

(12) Ziebarth, R. P.; Corbett, J. D. *Inorg. Chem.* **1989**, *28*, 626.
(13) Zhang, J.; Corbett, J. D. Unpublished research.
(14) *SDP User's Guide*; Enraf-Nonius, Delft, Holland, and B. A. Frenz & Associate, Inc., College Station, TX, 1988.
(15) Sheldrick, G. M. SHELXS-86. Universität Göttingen, Germany, 1986.
(16) Zhang, J.; Corbett, J. D. *Z. Anorg. Allg. Chem.* **1991**, *598/599*, 363.

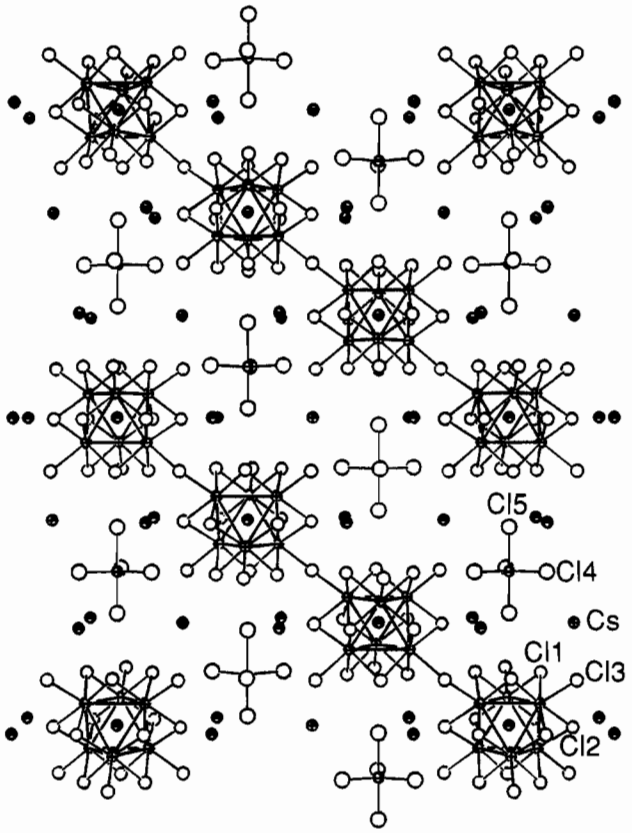

Figure 1. [110] projection of the structure of $Cs_3(ZrCl_5)[Zr_6(Mn)Cl_{12}]Cl_{6/2}$ ($R\bar{3}c$, hexagonal setting, $\vec{c}$ vertical, 90% probability displacement ellipsoids, with Cs and Mn shaded). The intercluster $Cl^{a\text{-}a}$ bridge bonds are included.

The $[Zr_6Cl^i_{12}Mn]$ cluster units are very similar to those found in two other 18-electron (closed shell[17]) compounds, $LiZr_6Cl_{14}Mn$[9] and $Li_2Zr_6Cl_{15}Mn$,[5] in terms of the Zr−Zr, Zr−Mn, and Zr−Cl^i (Zr−Cl1, Zr−Cl2) distances. The Zr_6 trigonal antiprisms are elongated along $\vec{c}$, but not severely in the sense that Zr−Zr distances differ by only 0.8% (0.0277 Å, 35σ), and the deviation of the Zr−Mn−Zr angles related by the 3-fold axes from 90° is minor, 89.57(1)°. This small distortion can probably be rationalized as a matrix effect arising from the presence of both more and closer Cs^+ ions around the cluster waist together with some expansion of the bridged network along c necessary to provide room for Cs^+ and $ZrCl_5^-$.

Likewise, the backbone of the structure, the $[Zr_6Cl^i_{12}Mn]$-$Cl^{a\text{-}a}_{6/2}$ network, has the same connectivity as each of those in cubic Nb_6F_{15}[8] and its stuffed analogue $Li_2Zr_6Cl_{15}Mn$[5] in terms of ring size. The earlier studies of $Li_2Zr_6Cl_{15}Mn$ also showed that lithium is the largest cation that would fit between interpenetrating nets.[5] Thus the two identical interpenetrating, but not interconnected, $Zr_6Cl_{12}(Mn)Cl_{6/2}$ nets in the last phase have been reduced to a single one in the present structure. The large voids that would be left are compensated by both a twist of the single net, with a substantial bending at the bridging $Cl^{a\text{-}a}$ (below), and the insertion of $ZrCl_5^-$ and Cs^+ props to hold this open. The remarkable result is that three features, the drive to achieve the optimal 18-electron $Zr_6Cl_{12}Mn$ cluster, the three-dimensional network required by the 6−15 stoichiometry, and the two Cs^+ cations necessary for the isoelectronic $Cs_2Zr_6Cl_{15}$-Mn plus the novel added ion pair $Cs^+ZrCl_5^-$, can all be accommodated within a single distorted ReO_3-like network. These are not sufficient conditions, of course, and a certain fortuity is also involved, especially regarding $ZrCl_5^-$ and the noteworthy "fit" of all of the components.

The volume reduction accompanying this change is appreciable, from 1107 Å^3 for two formula units in $Li_2Zr_6Cl_{15}Mn$ to 843 Å^3 here for the single similar network plus all of the counterions. A significant change in the distance of Zr−$Cl^{a\text{-}a}$ links is not seen, from 2.7281(7) Å to 2.7618(6) Å here; rather, the Zr−$Cl^{a\text{-}a}$−Zr bridges become bent, from 180 to 133.4(1)°. The $Cl^{a\text{-}a}$−Zr1−Mn arrangement in the exo link, which would be linear in the ideal situation, is also slightly bent to 177.5(4)° and may reflect the stretch of both the network (below) and the cluster antiprisms along $\vec{c}$.

Such a "trigonal twist" of the cubic ReO_3 cell ($Pm\bar{3}m$) along the [111] diagonal has been well described for a number of rhombohedral ($R\bar{3}c$) MF_3 phases, RhF_3 being close to the ideal.[18,19] The result retains the $MF_{6/2}$ connections in four-membered rings and achieves hcp fluoride. A much more open lattice pertains when M_6X_{12} clusters replace Re in cubic ReO_3, or M in rhombohedral MF_3, and this allows either pairs of identical lattices in Nb_6F_{15} or much more room for ion "fillers" in $Cs_3(ZrCl_5)Zr_6Cl_{15}M$ and $Cs_3Zr_6Br_{15}C$.[7] Focus on the dominant cluster "cations" is now more appropriate structurally, and these are seen to be cubic-closed-packed in projection (Figure 1). The twist transformation of a single $Nb_6F_{12}F_{6/2}$ net (ReO_3 cell) [about 111] into the observed $(Zr_6(Mn)Cl_{12})Cl_{6/2}$ array is illustrated in Figure 2. (The 12 inner halides are omitted in both parts cases for clarity.) The latter arrangement again achieves close to hcp packing of $Cl^{a\text{-}a}$, which would require 120° angles at $Cl^{a\text{-}a}$ to be exact. Actually, inclusion of a second slab of three cluster layers with the opposite orientation (via a glide parallel to c, Figure 1) is necessary to gain a coherent bridging pattern along $\vec{c}$ (the central cluster element is no longer spherical). Thus, pairs of cells along [111] are necessary, with twists of the double rhombohedra in opposite directions. This is better illustrated in Figure 3 for two primitive lattices from Nb_6F_{15} (left) and the observed $Zr_6Cl_{15}Mn$ (right), the clusters now being represented by the larger spheres. Although the result shown here was achieved by keeping the $X^{a\text{-}a}$ atoms about the central cluster that lies on the trigonal axis fixed, it could be illustrated just as well with the clusters fixed in space and the bridging halogens bending off the intercluster axes in the same manner. The actual structure achieved includes an elongation along $\vec{c}_H$ (the quasicubic [111]) such that the rhombohedral angle α_R is now 85.7°, not the 90° for cis-bridges in Nb_6F_{15}, and the c dimension is about 6.7% greater than the cubic ideal ($2\sqrt{3}a_R$ = 32.826 Å).

An even more encompassing classification is achieved when it is noted that the isolated trigonal $ZrCl_5^-$ clusters are centered at 0, 0, 0.25, i.e., half of the ccp layer repeat and the body center of the parent cubic or rhombohedral cell (Figure 3). This means that the $[Zr_6(Mn)Cl_{12}](ZrCl_5^-)Cl_{6/2}$ component corresponds directly and respectively to an ABX_3 perovskite, specifically a tilted rhombohedral ($R\bar{3}c$) example in which equal (small) tilts have occurred in the pseudocubic directions (along [111]), $a^-a^-a^-$ in Glazer's notation.[20]

Further consideration of the present structure, beyond obvious size effects, illustrate how and why the ion inclusions are different from those in classic perovskites. The anionic charge disposition of all members of the quasi-perovskite (ABX_3) network $(Zr_6Cl_{12}Mn)^{2-}(ZrCl_5^-)Cl^{a\text{-}a}_{6/2}$ is compensated by three counter-charged Cs^+ ions that sheath or screen particularly the

(17) Hughbanks, T.; Rosenthal, G.; Corbett, J. D. *J. Am. Chem. Soc.* **1988**, *110*, 1511.

(18) Babel, D. *Struct. Bonding* **1967**, *3*, 1.

(19) Wells, A. F. *Structural Inorganic Chemistry*, 5th ed.; Clarendon Press: Oxford, U.K., 1984; p 66.

(20) Glazer, A. M. *Acta Crystallogr.* **1972**, *A31*, 756; **1975**, *B28*, 3384.

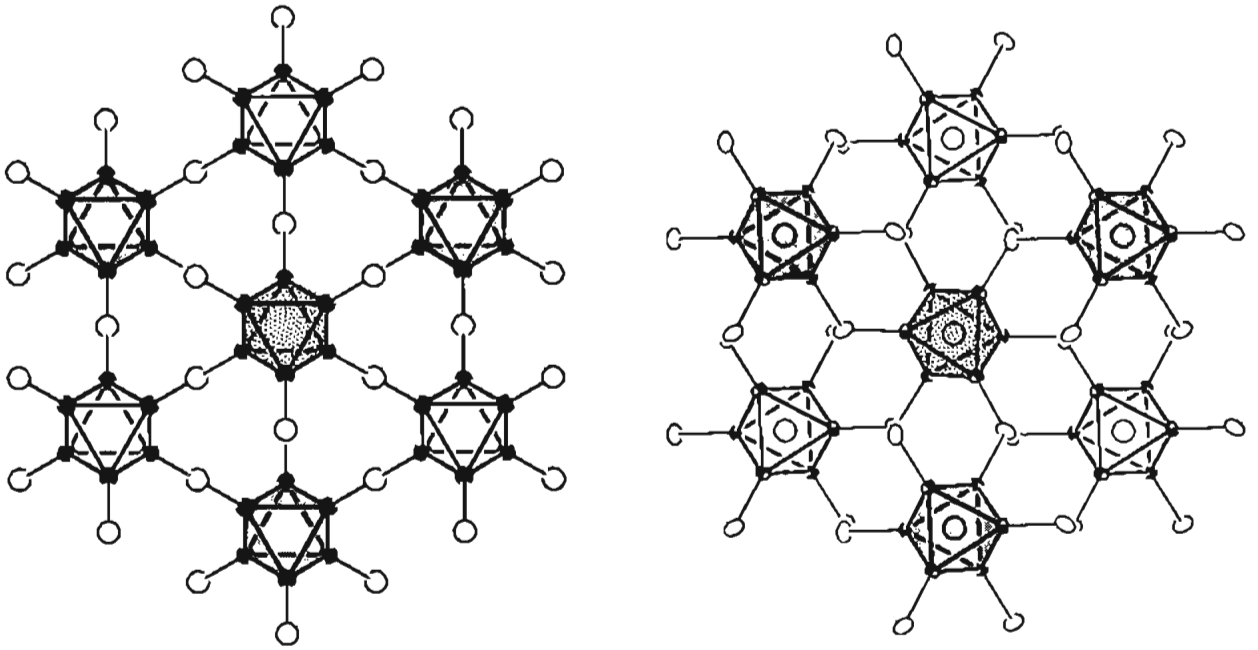

Figure 2. Comparison of X^{a-a} linkages of ccp clusters as viewed along the $\bar{3}$ axes in (left) one ReO_3-like network in Nb_6F_{15} [111] and (right) in $Cs_3(ZrCl_5)Zr_6Cl_{15}Mn$ [001], relative to a fixed central cluster. The inner halogen atoms on all the clusters are omitted for clarity, and the depth is emphasized by shading the clusters in the closest layer.

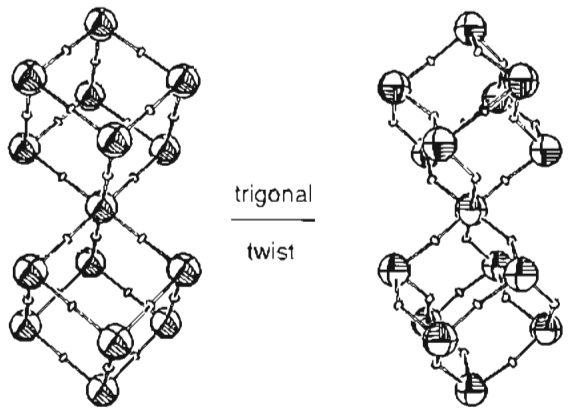

Figure 3. Trigonal twist that carries a pair of primitive (ReO_3-type) lattices in Nb_6F_{15} (left) into the double rhombohedral cell of $(Zr_6(Mn)Cl_{12})Cl_{6/2}$ (right). Large spheres in each case represent the ccp clusters.

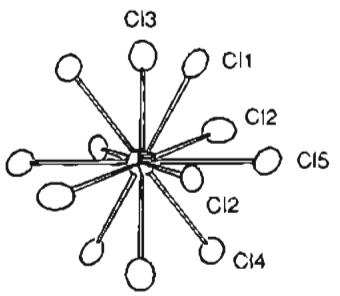

Figure 4. Cs^+ environment in $Cs_3(ZrCl_5)Zr_6Cl_{15}M$. The ion sits on an inversion center (90%).

first two ions. The cesiums are equivalent and appear well-bonded by 12 Cl neighbors (d(Cs−Cl) = 3.58−3.87 Å, $\bar{d}$ = 3.69 Å = $\sum CR$[21]), as shown in Figure 4. Half of these are Cl^i (Cl1, Cl2) and the other half, the more basic $Cl3^{a-a}$ and Cl4, Cl5 on $ZrCl_5^-$. Likewise, each $ZrCl_5^-$, with local D_{3h} symmetry is surrounded by six cesium ions and contains average (Zr−Cl) distances of 2.40 Å ($\sum CR$ (CN 6) = 2.47 Å[21]). The axial distances to Cl5 are 0.05 Å longer, perhaps because these anions are withdrawn from the adjoining Cs_3 environment (below).

Some additional layering is to be noted as well. The 12 horizontal layers per cell evident in Figure 1 (as opposed to the cp AX_3 layers which appear edge-on and tilted at ~38°) are also close-packed in style and stacked in a double ccp manner (neglecting cluster shape). Pairs of layers that contain only chlorine (Cl1, Cl3, Cl4) lie at the top and bottom of all clusters and through the waist of $ZrCl_5^-$, and these alternate with layers through the clusters that are defined by one Mn, three Cs and eight Cl2 atoms. Only the apical Cl5 atoms on $ZrCl_5^-$ deviate significantly from the latter layers, being displaced toward the Zr2 center by 0.49 Å.

The presence of the $ZrCl_5^-$ unit, seen in its local environment (without second nearest neighbor Cl^i) in Figure 5, is a most intriguing feature of this structure as it is believed to be the first example of a trigonal bipyramidal halogen configuration about Zr^{4+}. An important aspect of its stability must be the very good fit in the network. The fact that the $ZrCl_5^-$ group does not share any Cl atoms with the cluster network is at present unique, since in all published examples halide is always a member of a cluster or its bridged network. For instance, the six chlorine atoms around the isolated Zr^{+4} ion in the double salt structure $K_2ZrCl_6{\cdot}Zr_6Cl_{12}H$[22] and in related phases[10] also serve as terminal Cl^a to the cluster. From this point of view, the present compound is a double salt $CsZrCl_5{\cdot}Cs_2Zr_6Cl_{15}Mn$ with two complex anions that are truly independent of each other but compactly interspersed. (Compare the related $Cs_3Zr_6Br_{15}C$ in which a fractional pair of Cs^+ fill the $ZrCl_5^-$ hole.[7]) The present observations again emphasize the structural resemblance frequently found between the complex cluster and simple salt systems, despite their obvious differences in chemical compositions and bonding features. It also demonstrates the sophisticated ways that matter can be organized in the solid state. Finally, as summarized in the previous article,[6] the results also

(21) Shannon, R. D. *Acta Crystallogr.* **1976**, *A32*, 751.

(22) Imoto, H.; Corbett, J. D.; Cisar A. *Inorg. Chem.* **1981**, *20*, 145.

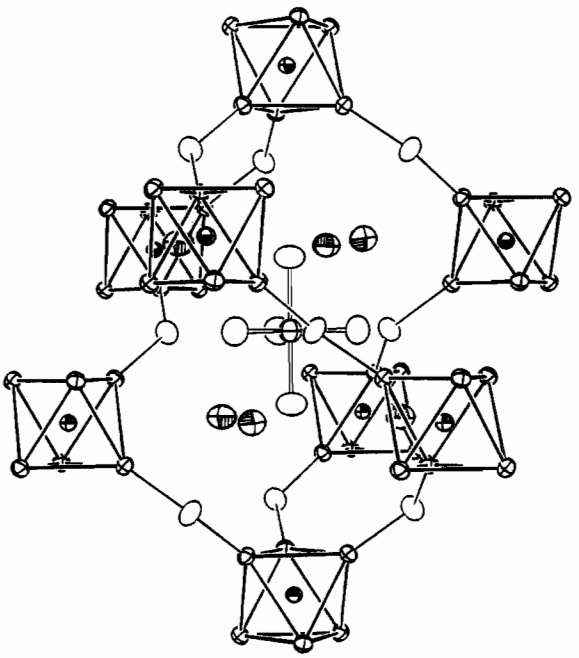

Figure 5. The $ZrCl_5^-$ anion together with the neighboring Cs^+ cations (shaded) and the $Zr_6Cl^{a\text{-}a}{}_{6/2}$ environment (3-fold axis vertical; 90% ellipsoids).

demonstrate a sixth independent way in which $M_6X_{12}X_{6/2}$ (or $M_6X_8X_{6/2}$) networks can be structured, in response to size variables of Z, X and the number and nature of any countercations.

The search for transition-metal-centered Zr_6Cl_{12}-type clusters has to date provided a family of clusters with Nb_6F_{15} structure or its stuffed modifications[5] together with a group of compounds with a defect superstructure of the $CsKZr_6Cl_{15}B$ (modified $CsNb_6Cl_{15}$) type.[3,12] Manganese is the lightest transition metal that has been incorporated into Zr_6Cl_{12} cluster systems, and it seems to behave differently from Fe and Co. No Mn analogue with a structure related to $CsKZr_6Cl_{12}B$[3] has been observed, and $Cs_3(ZrCl_5)Zr_6Cl_{15}Mn$ remains the only known metal-centered cluster compound of its type. Although it is possible that these distinctions are coincidental, or false because of a limited number of experiments, they are at present puzzling. Since $Li_2Zr_6Cl_{15}Mn$ (stuffed $Zr_6Cl_{15}Co$) does exist, it is difficult to imagine that the electronic state or size of Mn prevents compounds with it in the same structure types as the rest of the transition-metal-centered clusters. Very restrictive packing requirements regarding the size and number of countercations may be involved. On the other hand, limitations in cluster phases that arise from the greater stability of alternate noncluster compounds of the interstitial component may be responsible, as these often change in distinctive ways, even between neighboring transition metals.

Acknowledgment. This work was supported by the National Science Foundation, Solid State Chemistry, via Grants DMR-8902954 and -9207361 and was carried out in the facilities of Ames Laboratory, U.S. Department of Energy.

Supplementary Material Available: Tables of data collection and refinement details and the anisotropic displacement parameters (2 pages). Ordering information is given on any current masthead page.

IC941255E